Plasma Spray Joining of Al-Matrix Particulate Reinforced Composites

Composite spray powders are used in an attempt to produce true composite joints

BY T. ITSUKAICHI, T. W. EAGAR, M. UMEMOTO, and I. OKANE

ABSTRACT. Aluminum matrix composite joints have been produced on both aluminum alloy and metal matrix composite (MMC) substrates using powders containing SiC and Al_2O_3 particulates. Most of the composite powders were produced by ball milling, but the most effective joints were produced using Osprey composite powders. The results of preliminary joining experiments indicate that the substrate should be preheated to 200°C and a very wide bevel angle should be provided in order to obtain the highest strength joints. Silicon alloy additions to the matrix significantly improved strength but titanium additions had no effect. Heat treatment after spraying significantly improved the bond strength and restored precipitation hardening in the matrix. Significant amounts of Mg were lost from the deposit during spraying while some free silicon was produced by pyrolysis of the SiC powder; hence, further efforts must develop powder compositions that produce the optimum matrix composition in the sprayed deposit. Hot isostatic pressing of the samples to eliminate porosity had only a small effect on the final strength of the joints. No significant amount of Al_4C_3 was detected in deposits which contained SiC.

T. ITSUKAICHI is Chief Engineer at Shiojiri Works at Soga Shiojiri-Nagano, Japan. M. UMEMOTO is a Professor in the Production Systems Engineering Dept., Toyohashi University of Technology, Toyohashi, Japan. I. OKANE retired from Toyohashi University in 1995 and is now Professor Emeritus. T. W. EAGAR is Head of the Materials Science and Engineering Department at Massachusetts Institute of Technology, Cambridge, Mass.

Introduction

Interest in metal matrix composites (MMC) such as SiC/Al and Al_2O_3/Al (SiC and Al_2O_3 in a matrix of aluminum, respectively) is currently expanding because of the improved performance offered by these advanced materials. However, the utilization of MMC is presently limited by their poor weldability when using conventional fusion welding processes (Refs. 1, 2). Exposure of the SiC/Al-type composite to temperatures above the liquidus of the aluminum alloy, as typically experienced in welding, results in a severe loss of engineered properties due to the formation of brittle and hygroscopic aluminum-carbon compounds (Refs. 2, 3), typically Al_4C_3. Furthermore, conventional fusion welding produces a weld pool that has poor fluidity and that solidifies with large volumes of porosity in both the weld and the heat-affected zone (HAZ) because of the release of hydrogen emanating from the aluminum powder used to fabricate many MMCs. Ahearn, *et al.* (Ref. 1), clearly demonstrated that vacuum degassing for long periods of time prior to welding did reduce porosity in welds deposited by GTAW, but Al_4C_3 and Al-Si eutectic were detected in the degassed composites.

KEY WORDS

Plasma Spray
Al-Matrix Composites
Particulate Composites
Ball-Milled Powders
Spray Deposit Powder
Preheating
Al-Si-Ti Powders
2014 Al Powders
SiC Particulates
Hot Isostatic Pressure

Nothing has been reported on the joining of composites by the nontransfer thermal spraying technique. Although this technique has been commonly used for surface coating to improve wear resistance, heat resistance, and corrosion resistance of metals and alloys, it seems that few researchers thought that it would be a successful technique to join these composite materials directly. It may be that excellent weldments of MMC could be obtained by this technique if good adhesive and cohesive bonding of the sprayed deposit were accomplished, for it is believed that few brittle compounds, such as Al_4C_3, little porosity, and almost no HAZ would form in the joints since the surface of the substrate doesn't melt during spraying due to the small heat input into the joints. The sprayed deposit properties may be enhanced if a distinct second phase material, such as ceramic fibers, whiskers, particulates, or monofilaments, is incorporated into the deposit structure (Ref. 4).

This project was designed to develop manufacturing technology of plasma spray joining methods for MMC of both SiC/Al and Al_2O_3/Al. This may be the first study of the nontransfer plasma spray joining processes utilizing composite spray powders to attempt to produce true composite joints containing unreacted SiC or Al_2O_3 particulates with properties more closely matching those of the composite base metals. In this study, conventional (unreinforced) 6061

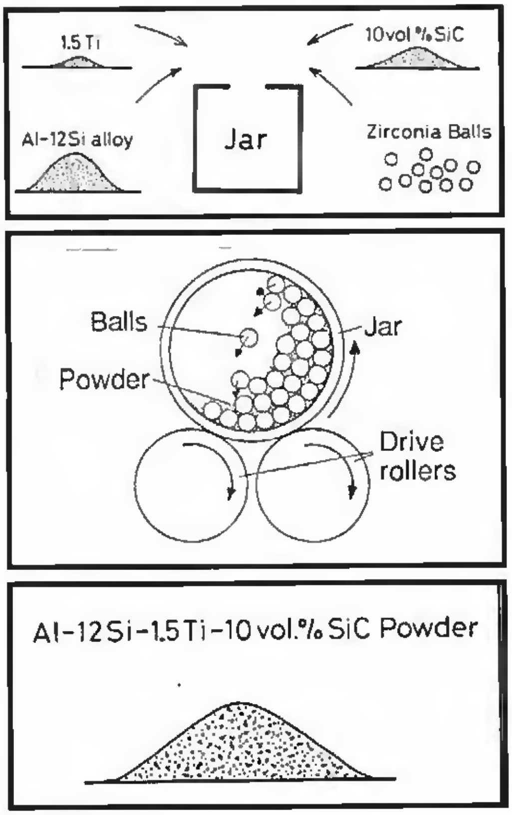

Fig. 1 — Ball milling was used to prepare the composite spray powders. The aluminum alloy reinforcing phase and any other additive elements were combined in this process.

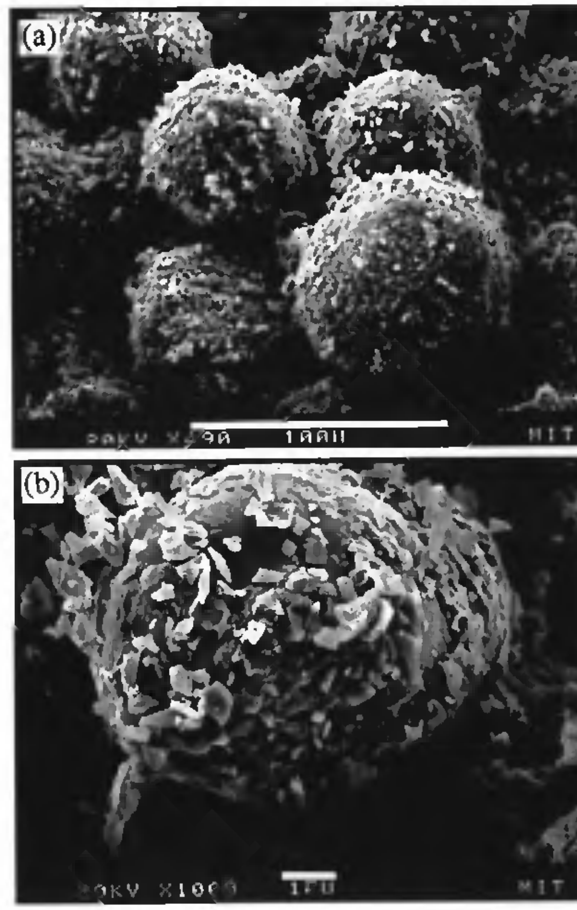

Fig. 2 — SEM photos of ball-milled Al-12wt-%Si-1.5wt-%Ti-10vol-%SiC with 5-μm SiC. A — 490X; B — 1000X.

Al alloy base plates were used for simplicity and economy.

Two matrix alloys were used with the composite spray powders, namely, Al-Si-Ti alloy and 2014 Al (Al-Cu-Si-Mg) alloy. In the former, Si additions were made 1) to reduce the melting temperature of the Al matrix alloy of the composite powder for ease of fusion during spraying, 2) to reduce the extent of reaction between Al and SiC (Refs. 2, 5, 6) in the sprayed deposit, and 3) to prevent liquid alloy particles from oxidizing. Reactive metal additives, such as Ti, were intended 1) to prevent the formation of Al_4C_3 (by the reaction between SiC and Al) by forming reactive metal carbide protective layers on SiC, which are inert with respect to Al (Ref. 6) and 2) to improve the wettability between SiC and Al (Ref. 6). Yang (Ref. 6) thermodynamically explained the above effect of Si and Ti additions.

Strengthening treatments, such as HIP consolidation and solution/aging heat treatment, were performed on the sprayed joints. Furthermore, a comparison of the effects of ball-milled 2014 Al-SiC powder and Osprey 2014 Al-SiC powder was made.

Table 1 — Spray Materials

1 Al powder (99.0% 45–90 μm)
2 Al-x wt%Si-y wt%Ti-z vol%SiC ball-milled powder (45–150 μm)
x: 0, 6, 12, 20 (wt-%)
y: 0, 0.5, 1.5, 3.0 (wt%)
z: 0, 5, 10, 15 (vol%) . . . . . . mainly, 10 vol-%SiC . . . . . .
Three types of SiC powders used

Particle size (μm)	Purity (%)	Remarks
5	99.5	Cerac Inc.
15	98.0 (min.)	Norton
40	98.8	Alfa Products

3 Al-a wt%Si-b wt%Ti-10 vol%Al_2O_3 ball-milled powder (45–150 μm)
a: 0, 6, 12 (wt%)
b: 0, 1.5, 3.0 (wt%)
Al_2O_3 (20 μm, 99%, METCO Inc.)
4 2014 Al-15 (vol%SiC (15 μm) Osprey powder (45–150 μm)
5 2014 Al-c vol%SiC (5, 15 μm) ball-milled powder (45–150 μm)
c:0, 5, 10, 15 (vol%)
6 2014 Al ball-milled powder (45–150 μm)
Mg content: 0.5, 1.5, 3.0, 5.0 (wt%)

Metal powders for ball milling
Cu powder (99.0%, 45-90 μm), Ti powder (99.0%, <45 μm)
Si powder (99.0%, <45 μm), Mg powder (99.8%, <45 μm)

Experimental Materials

Spray Powders

Table 1 shows the spray powder formulations which were prepared by ball milling or spray deposition. Three types of SiC were used with 5-, 15-, and 40-mm average size, respectively. The Al_2O_3 powder had a 20-mm average size, while the aluminum metal powder was spherical with an average size of 45 to 90 mm.

Substrates

The substrates used in this study were 1100 Al-O, 6061 Al-T4, 10 vol-% Al_2O_3/6061 Al, and 20 vol-% SiC/6061 Al-O. Typical tensile properties are shown in Table 2. The thickness of these plates was 3.2 mm (1/8 in.) and the joint bevel angle was large (130 deg, no root opening).

Table 2 — Substrates and their Tensile Properties

Substrate	UTS (MPa)	0.2% proof stress (MPa)	Elongation (%)
1100 Al-O[a]	82.5	35.3	35.0
6061 Al-T4[a]	240.1	145.0	22.0
10vol%Al_2O_3/6061Al[a]	355.1	315.1	6.3
20vol%SiC/6061Al-O[a,b]	231.7	142.7	13.7
20vol% SiC/6061Al-T6	272.1	232.1	15.4
20vol%SiC/6061Al-T8	300.3	276.2	13.2
20vol%SiC/6061Al-T9	347.8	323.7	14.9

(a) Substrate used in this study.
(b) As rolled (longitudinal properties).

Experimental Procedure

Description of Apparatus

A commercial nontransferred arc spraying system was used. To increase the effectiveness of the deposit rate and the thickness, the plasma gun was mounted vertically and operated from a pneumatically controlled table. To increase the reliability and accuracy of a controlled deposit thickness, the gun was positioned in a stationary location. The vertical axis (Z) was controlled by raising and lowering the table. This is how the depth of field of the gun was controlled. In the joining process, the gun was moved right to left repeatedly on the horizontal axis (X) at translational speeds of 12.5 m/minute during spraying.

Preparation of Spray Powders

Most of the composite spray powders were prepared by ball milling Al alloy powder with the SiC or Al_2O_3 particulate reinforcing phase and any other additive element powders without any additional agents — Fig. 1. To a considerable extent, this formed a homogeneous composite powder wherein the hard phase was dispersed in the soft alloy matrix of the composite. The ball milling conditions are shown in Table 3. When SiC or Al_2O_3 particulates were incorporated into the composite metal powders, these were added at the start of the milling process. Figures 2 and 3 show SEM photos of the ball-milled Al-12wt-%Si-1.5wt-%Ti-10vol-%SiC (5 mm) powder and the ball-milled 2014 Al-10vol-%SiC (15 mm) powder, respectively, as examples.

Osprey composite SiC powder in a 2014 Al alloy matrix, as well as the ball-milled composite powder, was used in this study. The 2014 Al alloy was melted by induction heating in a crucible. The crucible was pressurized and the metal was ejected through a nozzle into an atomizer. SiC powder was injected into the metal spray. Figure 4 shows SEM photos of the 2014 Al-15vol-%SiC Osprey powder. The SiC particulates are incorporated into the metal powders more deeply and homogeneously than those of ball-milled composite powders.

Figure 5 (Ref. 7) shows the particle size distribution of the Osprey powder. The range between 45 and 150 mm represents where SiC particulates were incorporated into the metal droplets. To separate the unreinforced particles the Osprey powder measuring between 45 and 150 mm was separated from the finer powders and then used in this study.

Table 3 — Ball Milling Conditions

Mill jar	Alumina vial (1.8 liters)
Milling media	Zirconia ball (12.7mm radius end cylinder)
Atmosphere	Argon
Media to powder weight ratio	10:1
Milling time	2–3 hours
Mill speed	76–80 rpm

Table 4 — Substrate Surface Blasting Conditions

Air Pressure	0.31MPa
Blasting Material	Siliceous Sand
Grit Size	20-50 mesh
Blasting Distance	100mm
Blasting Angle	45°-90°
Blasting Time	1 minute

Determination of Spray Conditions and Spray Joining Processes

Grit Blasting

Figure 6 shows a joint specimen and its dimensions. Before joining, the shaded portion to which a sprayed deposit would adhere was roughened by

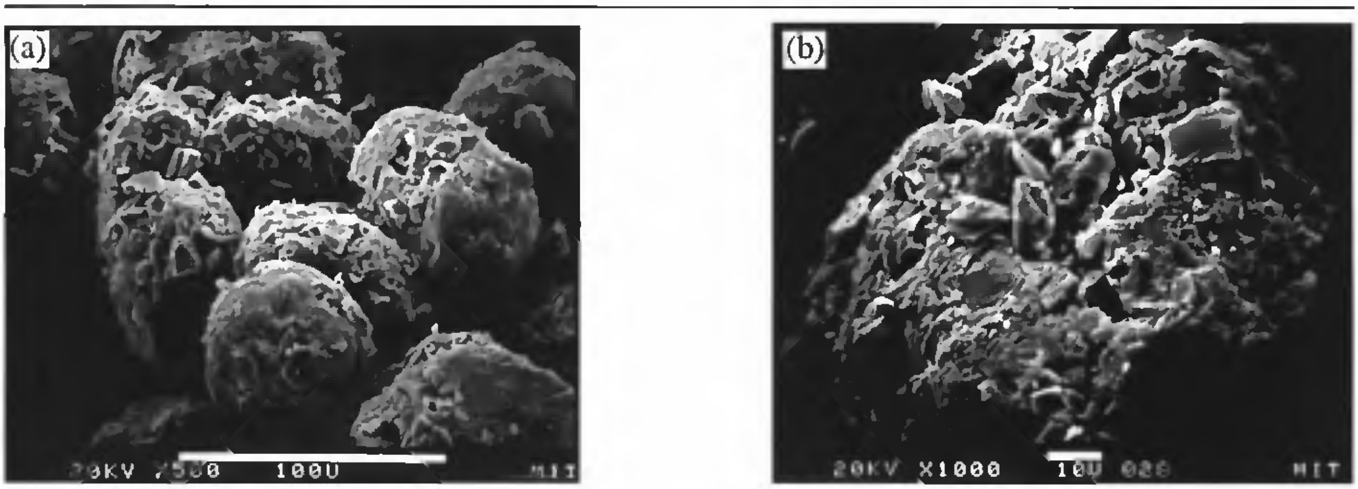

Fig. 3 — SEM photos of ball-milled 2014 Al-10vol-%SiC with 15-μm SiC. A — 500X; B — 1000X.

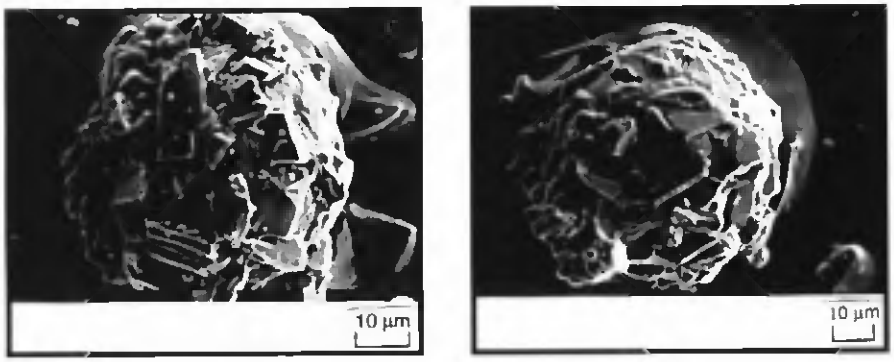

Fig. 4 — SEM photos of 2014 Al-15vol-%SiC Osprey powder, which was melted, pressurized, and atomized to form the powder.

abrasive grit blasting. This was done to clean the oxides from the surface and provide a rougher surface for better adhesion. Blasting conditions are shown in Table 4.

Preheating

To determine the optimum preheating temperature of the substrate, tensile tests of preliminary spray-joined specimens were performed — Fig. 8. Tensile strength was measured by applying a tensile load to the sprayed specimen vertically to the axis of spraying. The reported joint efficiencies were normalized by the formula: Joint Efficiency (%) = 100 X (UTS of the joint)/(base plate longitudinal UTS). Figure 7 shows three types of failure after tensile tests. Mode A is an adhesive fusion line failure. Mode C is a cohesive failure wholly in the deposit metal. Mode B is a mixed failure.

As seen in Fig. 8, the tensile strength of joints increased with preheating temperatures up to 200°C. It is generally believed that preheating of the substrate is necessary 1) to eliminate moisture on the surface which prevents molten sprayed metal particles from adhering strongly to the substrate, 2) to prevent hot sprayed deposit from cooling rapidly, and 3) to allow the substrate to expand in order to decrease the relative difference of thermal expansion and contraction in volume between the substrate and the hot sprayed deposit. In this experiment, the tensile strength of joints tended to decrease above 200°C, which was due to excessive oxidation of the substrate during preheating. On the other hand, without preheating, easy spalling of the deposit from the substrate occurred. Wholly cohesive failures were obtained at 200°C.

Spray Distance

Figure 9 shows the influence of spray distance on deposit efficiency (DE) and ultimate tensile strength (UTS) of the joints. One of the spray powders was Al and the other was 2014 Al-15vol-%SiC Osprey powder. In the latter case, heat treatment as described in the upcoming section on "Strengthening Treatments of the Joints" was performed after joining. It is seen that bringing the spray gun near to the substrate with a narrow spray track resulted in greater deposit efficiency of deposited materials; however, the strength of the deposit decreased due to less bonding force between the particles or at the deposit-substrate interface. A 95-mm spray distance was chosen in this study as providing the best combination of deposit strength and deposit efficiency.

Bevel Angle

The influence of bevel angle (included angle) of the joint on the tensile strength is shown in Fig. 10. The larger the bevel angle, the greater the cohesive strength as well as the adhesive strength. It is believed that the increase of tensile strength with bevel angle resulted from greater impact force of the spray particles and a resulting decrease in pores in each deposit. A 130-deg bevel angle was selected for further work in this study.

Plasma Spraying Conditions

Based on the results of the preliminary tests as noted above and the recommended spray conditions (Ref. 8) from the equipment supplier, the plasma spray conditions of this study were determined as described in Table 5. It was found that all the substrates required preheating in order to obtain satisfactory results. The typical preheat time before spraying was 10 minutes.

Using these conditions, plasma spray joining tests using composite spray powders were carried out.

Table 5 — Plasma Spraying Conditions

Plasma arc gas	Argon
Powder carrier gas	Argon
Plasma arc gas flow	2.1m^3/hour (74.5CFH) at 0.35MPa
Powder carrier gas flow	0.14m^3/hour (5.0CFH) at 0.35MPa
Arc current	500A
Arc voltage	30V
Spray distance	95mm
Gun translational speed	12.5m/minute
Preheating temperature of substrate	200°C
Bevel angle	130°

Table 6 — Chemical Analysis of 2014 Al-15vol-%SiC Osprey Powder and its Sprayed Deposit (wt-%)

	Al	Si(a)	Si(b)	Cu	Mn	Mg	Fe	Ti	Zn
Powder	Bal.	0.99	12.25	3.51	0.60	0.37	0.37	0.033	0.013
Deposit	Bal.	2.89	7.92	3.64	0.61	0.31	0.40	0.037	0.009

(a) Soluble
(b) Insoluble.

Strengthening Treatments of the Joints

To increase the density and to greatly improve the adhesive and cohesive bonding of plasma sprayed deposits, HIP (hot isostatic press) and/or solution/aging heat treatments were carried out after joining. The HIP temperature, time, and pressure were 500°C, 1 hour, and 103.4 MPa (15,000 psi), respectively. The samples were not encapsulated before HIPing.

Heat treatment was added not only to strengthen the joint, but also to resolutionize the substrate because preheating (200°C 10 minutes) prior to joining brought about a 30% decrease in the tensile strength of the substrates. Therefore, the specimens were heat-treated to the T6 condition for 2014 Al (solution treatment: 500°C, 8 h/aging treatment:

160°C, 18 h) (Ref. 9). These treatments were also expected to remove residual stresses in the deposit.

Evaluation of the Joints

Tensile Tests

Tensile tests of all specimens were performed at room temperature. The tests were conducted in an Instron tensile testing machine at a crosshead speed of 0.02 cm/min (0. 008 in./min). All results represent an average of three or more tests.

Fracture surfaces were examined in the scanning electron microscope.

Metallographic Analysis

Representative samples were sectioned from the joint and mounted in bakelite. These samples were then mechanically polished to 0.3 mm finish. Some of them were etched lightly with Keller's reagent.

The volume fraction of the reinforcement phase and porosity in the sprayed deposits were measured using an image analyzer.

Measurement of the Al_4C_3 Concentration

Cross-sections of the deposits were cut to fit into the sample holder of an x-ray diffractometer. The samples were aligned so that the x-ray beam impinged on the joint region, which was exposed to the maximum heat input during the joining process. This arrangement resulted in the most intense signal when Al_4C_3 was present.

Results and Discussion

Joining Using Al-Si-Ti Alloy Matrix Composite Spray Powders

Spray Powders with SiC Particulates

A wide variety of composite metal powder formulations for spraying was prepared and used to produce demonstration joints for detailed evaluation and testing, and to select the most promising compositions. Figures 11 and 12 show the influence of Ti content in composite spray powders with 10 vol-%SiC particulates (5 mm and 40 mm average size, respectively) on UTS. Although addition of Ti had almost no effect, adding Si up to 12% had a beneficial effect on tensile strength of the joints. The fine Ti powder which was used in this study is very reactive as compared with other elements used. It is thought that Ti did not function well as an additive for improving the tensile strength through improved wetting of aluminum to the ceramic particles because of its excessive oxidation during ball milling and plasma spraying. On the other hand, it was found that 12 wt-%Si was the most effective addition in improving the joint strength.

In both Figs. 11 and 12, the joints with relatively high tensile strength tended to produce adhesive/cohesive mixed failure modes, which meant that bonding at the substrate-deposit interface was almost as strong as the particle to particle interlocking in the deposit.

The typical fracture surface of an Al-12wt-%Si-1.5wt-%Ti-10vol-%SiC (5-mm SiC) deposit exhibited some local ductile, dimpled morphology as shown in Fig. 13. There were many fine droplets that were ejected from the transferring particles and solidified in the deposit. These imperfections should be controlled by modifying the electric output power of the plasma gun equipment.

Figure 14 shows the effect of SiC particulate size on UTS and SiC incorporation efficiency. The SiC content in each deposit was generally smaller than the fraction of SiC in the starting powder. Most of the SiC particulates which disappeared, escaped from the stream of flying molten composite powder during spraying; probably because of poor wettability between the SiC and the molten Al alloy and poor incorporation of SiC particulates into the Al alloy matrix of the composite powder during ball milling. 15 mm SiC particulates tended to deposit more efficiently as compared with 5- and 40-mm SiC, because 15-mm SiC particulates were incorporated into the Al matrix powder more thoroughly by ball milling due to the relative SiC and Al particle size as shown in the upper illustration of Fig. 14. Nonetheless, the 15-mm SiC joints showed less strength than the other joints in spite of the larger volume of the reinforcement phase. That means that the SiC particulate functioned less effectively as a reinforcement phase and that the rule of mixtures does not apply directly. The larger the SiC paticulates in volume, the less the tensile strength is improved. There are several reasons why the strength values were low, among them, low bond strength at the SiC-Al alloy matrix interface and alteration of the chemical composition of the matrix during ball milling and plasma spraying.

An exception to the low strength of 15-mm SiC deposits occurs after heat treating. As seen in Fig. 15, the tensile strength tended to decrease with increasing SiC content in as-sprayed specimens except 10vol-%SiC (5-mm) deposit. Heat treatment after joining was done to strengthen the substrate and the interface between the substrate and the deposit. Heat treatment seemed to improve the bonding at the interface since all frac-

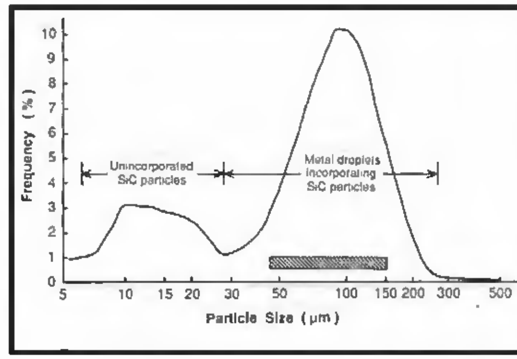

Fig. 5 — The particle size distribution of the Osprey powders. The smaller particles were principally SiC without aluminum metal.

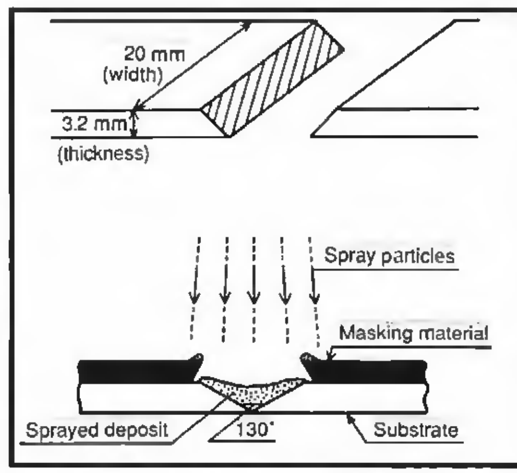

Fig. 6 — Specimen geometry and spraying procedure.

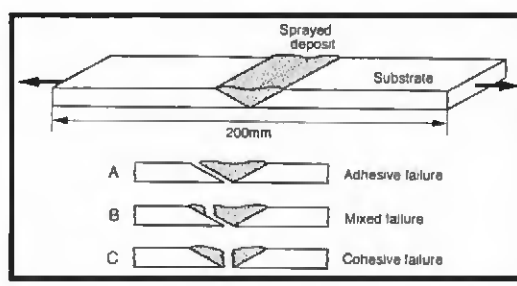

Fig. 7 — The three modes of failure were defined as adhesive, mixed and cohesive.

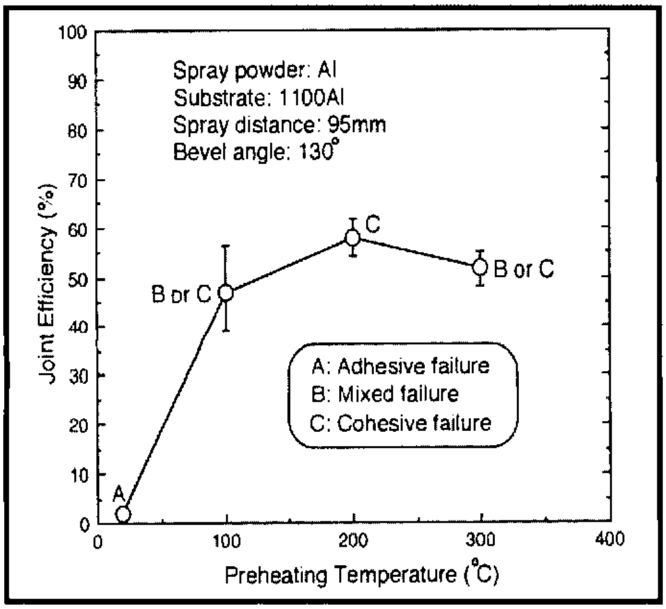

Fig. 8 — Joint efficiency, in terms of failure mode and strength, varied with preheating temperature. The highest strength occurred at 200°C in a cohesive failure mode.

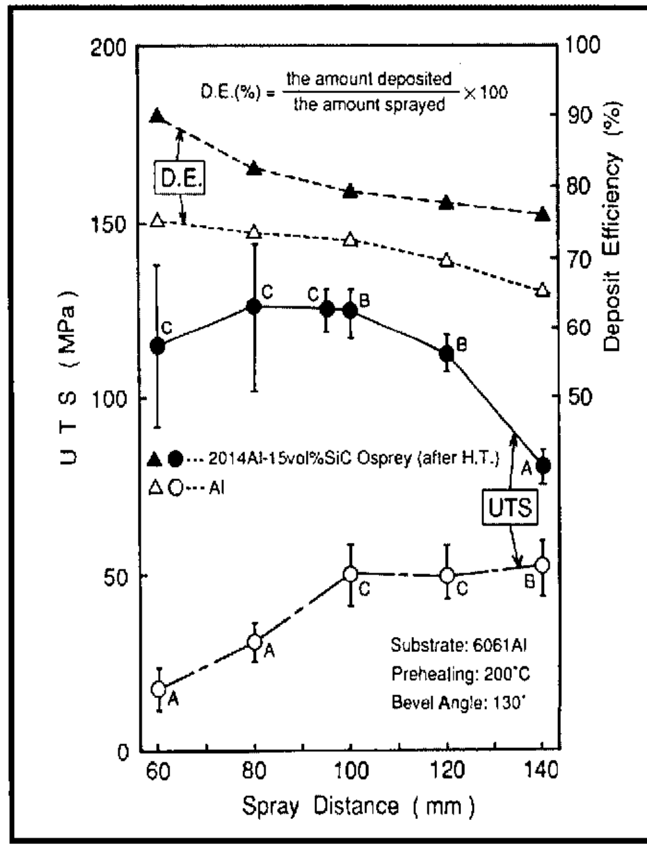

Fig. 9 — Spray distance affects both the deposit efficiency and the UTS. The best combination of properties was found at 95 mm.

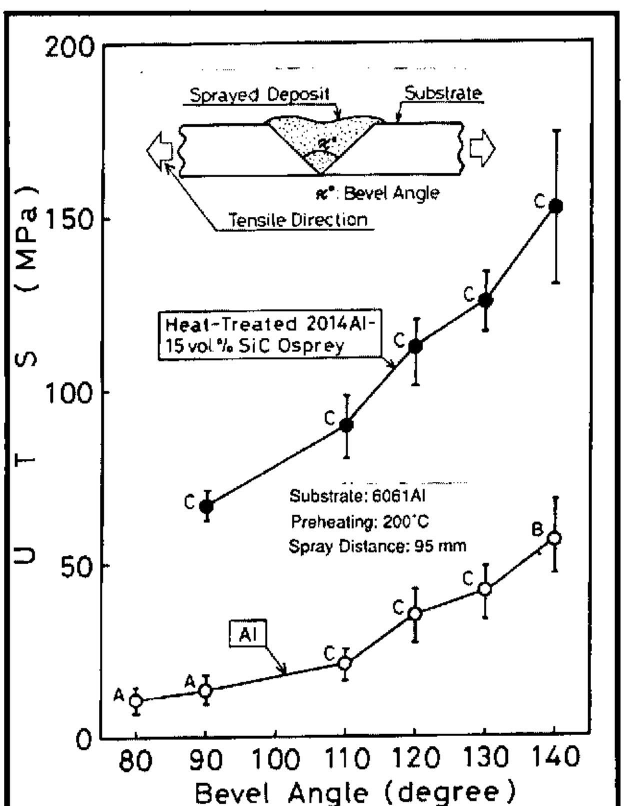

Fig. 10 — Increases in bevel angle increased the UTS, cohesive strength and adhesive strength. Larger bevel angles result in greater impact force of the droplets and less porosity.

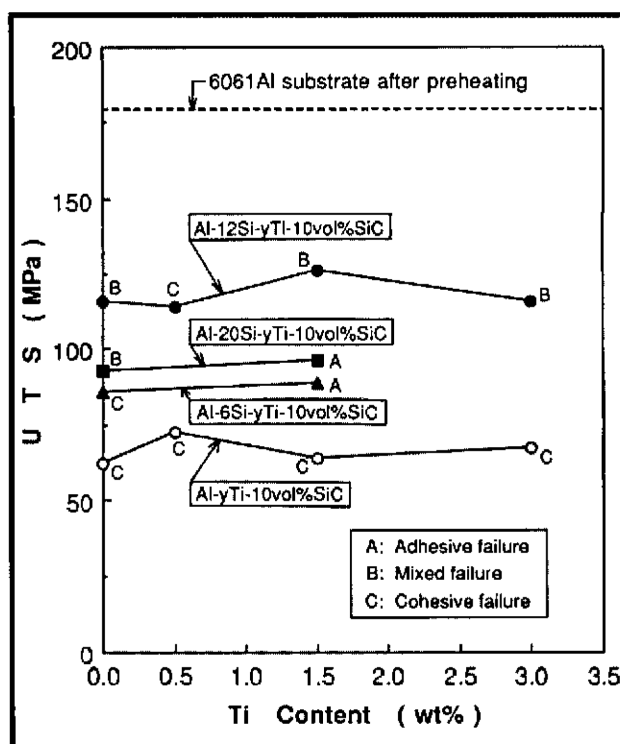

Fig. 11 — The tensile strength of composites sprayed with 5-μm SiC particles was not influenced by Ti content. Higher Si contents up to 12% Al-Si eutectic composition produced higher strength.

tures were type C (cohesion failure). In the case of joints with 15-mm SiC particulates, the heat-treated specimens were stronger than the as-sprayed specimens, because bond strength between the SiC phase and the Al alloy matrix appears to be improved by the heat treatment. Nonetheless, the final strength values were not very high because the deposits did not contain constituents which create strengthening by heat treatment.

Fujiwara (Ref. 10) reported that tensile strength (and modulus of elasticity) of MMCs increased with decreasing SiC particulate size. In this study, this tendency was true to a certain extent as seen in Figs. 14 and 15 (as sprayed).

Figure 16 shows microstructures of sprayed deposits with 5, 15, or 40 mm SiC particulates.

Based on XRD analysis, no Al_4C_3 phase was observed in the sprayed deposits. It is thought that since SiC particulates were in contact with the molten Al alloy particles for only a moment during plasma spraying, almost no reaction between SiC and molten Al alloy occurred.

Porosity varied from 1 to 4% in each deposit. These pores did not seem to influence the tensile strength and failure mode of deposits significantly.

Spray Powders with Al_2O_3 Particulates

As shown in Fig. 17, Si additions influenced the UTS much more than Ti content. The composition with the best joint strength was Al-6wt-%Si-1.5wt-%Ti-10vol-%Al_2O_3. As compared with spray powders with SiC particulates, however, the tensile strength was very low, although Al_2O_3 incorporation efficiency was high — Fig. 18. The Al_2O_3 content in sprayed deposits increased with the Si content.

Figure 19 summarizes the results of joint tensile strength for all the specimens joined using each spray composite powder.

Joining Using 2014A1-Matrix Composite Spray Powders

Strengthening Treatment Effect

Figure 20 shows strengthening treatments and their effect on UTS and joint efficiency. Figure 20B compares the tensile strength of five different specimens. Combination (E) using HIP and T6 heat treatment gave the highest tensile strength. As compared with as-sprayed joints (A), the strength improved dramatically (about 95%). Even without HIP, the T6 heat treatment (C) produced joints 60% stronger than those of as-sprayed specimens.

Chemical analysis of the 2014 Al-15vol-%SiC Osprey powder and its spray deposit is described in Table 6. The sprayed deposit contained much soluble silicon because of pyrolysis of some of the SiC particulates during plasma spraying. In the 2014 Al alloy, precipitation of intermetallic compounds, such as $CuAl_2$ and Mg_2Si improves the mechanical properties of the alloy. Suzuki, *et al.* (Refs. 11, 12), reported that Al-Mg_2Si alloys containing excess silicon have faster age-hardenability than the balanced alloy. Thus, it is thought that the excess soluble silicon content in the deposit brought about over aging, since the aging treatment followed the normal heat treatment for 2014 Al described in Ref. 6.

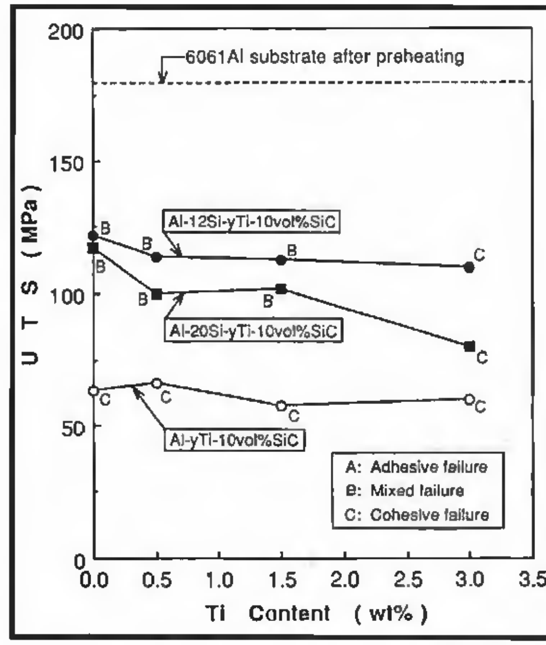

Fig. 12 — Mixed failure modes were observed at a variety of Ti contents for 40-μm SiC composite powders.

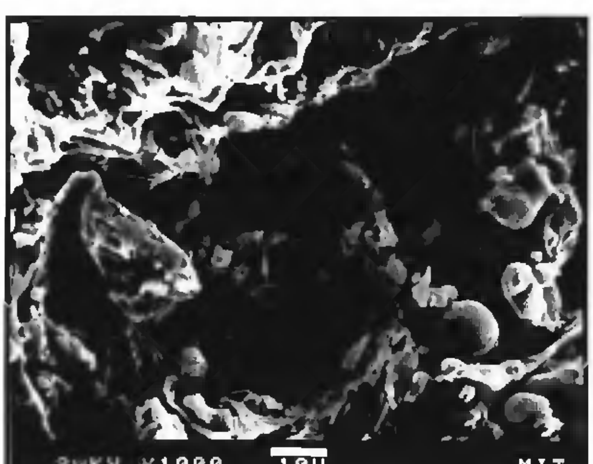

Fig. 13 — Some local ductile, dimpled morphology was found on the fracture surface of Al-12wt-%Si-1.5wt-%Ti-10 vol-%SiC (5-μm SiC).

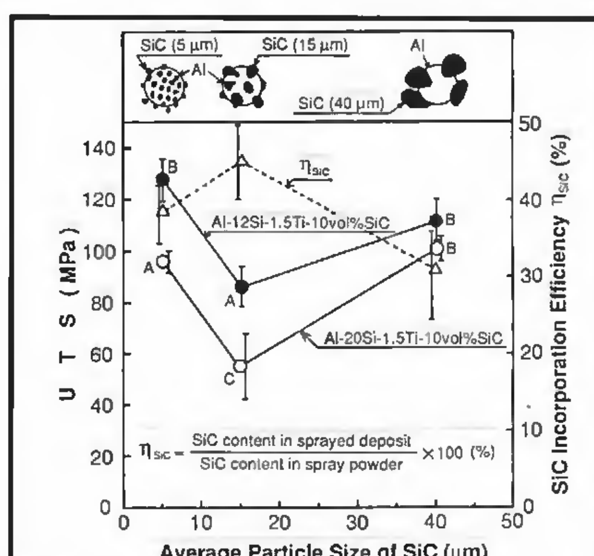

Fig. 14 — SiC incorporation efficiency and UTS vary with SiC particulate size. SiC was lost during spraying, probably because of poor wettability between the SiC and molten aluminum.

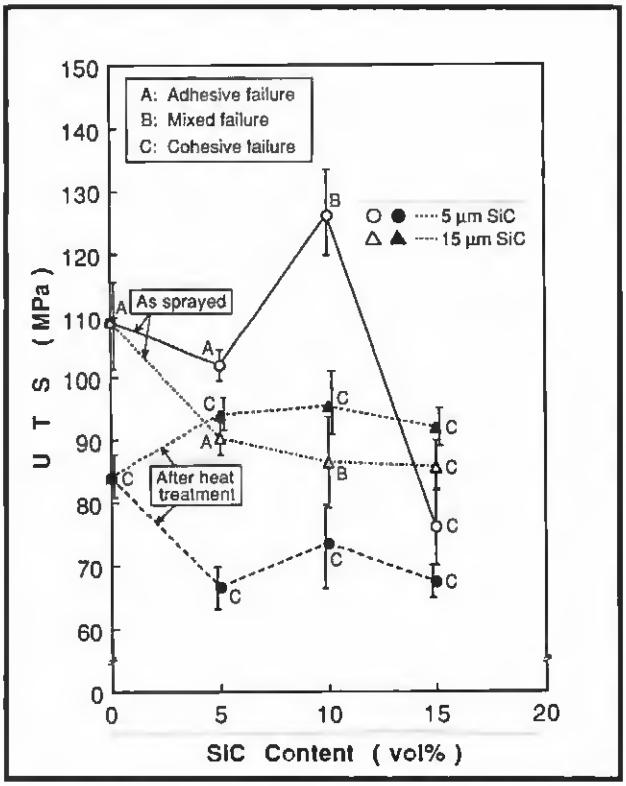

Fig. 15 — The tensile strength tended to decrease with increasing SiC content, and bonding improved during heat treatment since all the failures became cohesive.

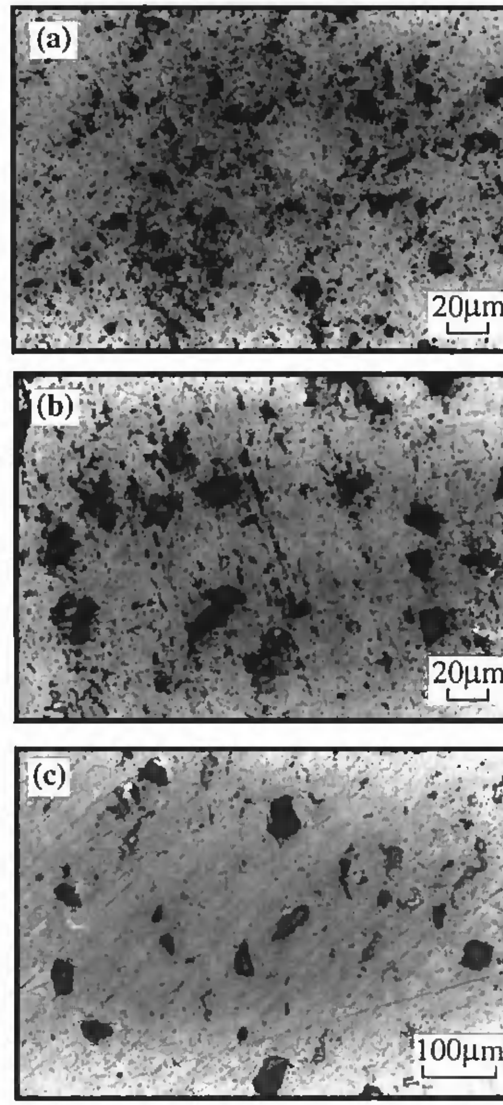

Fig. 16 — Microstructures produced with various size SiC particulates. A — 5 µm; B — 15 µm; C — 40 µm SiC.

Therefore, it is possible that higher strength could be obtained if optimum heat treatment conditions (especially aging time) were developed for these specimens. Porosity was 1 to 3% in each deposit.

Figure 21 shows the microstructures of the 2014Al-15vol-%SiC Osprey deposit. Apparently the uniformity of dispersion and incorporation of the SiC particulates in the Al alloy matrix were better than those of ball-milled 2014 Al15vol-%SiC deposits. The typical fracture surface of the heat-treated Osprey deposit exhibited a locally ductile, dimpled morphology as shown in Fig. 22.

Influence of SiC Content on UTS

Figure 23 shows the effect of SiC content in ball-milled 2014 Al-SiC composite spray powders on UTS. All the specimens were heat-treated before the tensile test. The strength generally tended to decrease with increasing SiC content. There are several possible reasons why the strength values were low, among them low bond strength at the SiC/Al matrix interface and alteration of the chemical composition of the matrix during ball milling and plasma spraying. Nonetheless, the Osprey composite powder containing 15vol-%SiC produced joints with better strength than that of ball-milled powder at the same SiC content. The deposit made of the Osprey powder showed higher SiC incorporation efficiency (h) as compared with ball-milled powders. Ball-milled powder with smaller size SiC (5 mm) also showed better strength values than that of the ball-milled powder with 15 mm SiC.

Joining of SiC/6061 Al and Al_2O/6061Al MMCs

Figure 24 shows results of the strengthening treatments of Osprey deposits on 6061 Al and 6061 Al-matrix particulate reinforced composites' (namely, 20vol-%SiC/6061 Al and 10vol-%Al_2O_3/6061 Al) substrates. Though the HIP treatment prior to the T6 heat treatment was very effective in improving the joint strength of the specimens with 6061 Al substrates, it did not produce much improvement in the strength of the specimens produced on MMC substrates. Figures 25 and 26 show the microstructures at the interfaces between the SiC/6061Al substrate and the sprayed Osprey deposit, and the Al_2O_3/6061Al substrate and the Osprey deposit, respectively. It is thought that the presence of SiC or Al_2O_3 phase on the surface of the MMC substrate to which a sprayed deposit would adhere, decreased the adhesive bonding at the deposit-substrate interface to a certain extent. Nonetheless, the adhesive or adhesive/cohesive mixed strength values of the specimens with SiC/6061Al substrates were a little higher than those of specimens with Al_2O_3/6061 Al substrates, although it should be noted that the former contained 20 vol-%SiC phase and the latter contained 10 vol-%Al_2O_3 phase. This suggests that the interface between the SiC phase on the surface of the substrates and the sprayed 2014 Al alloy had better adhesion.

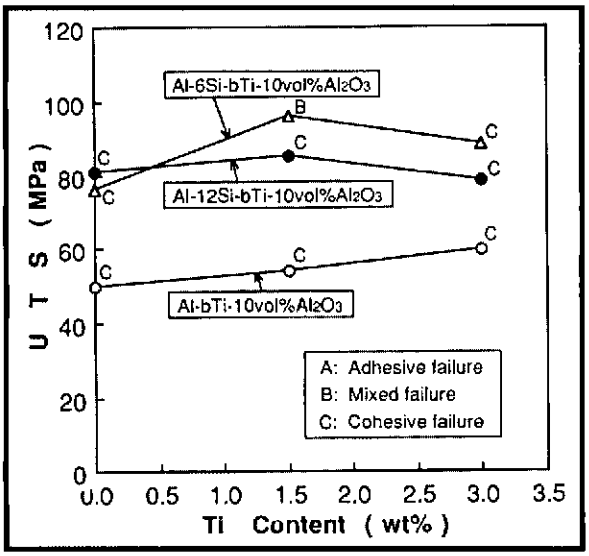

Fig. 17 — The Al-6wt-%Si-1.5wt-%Ti-10vol-%Al_2O_3 has the best joint strength, and Si additions had a greater influence than Ti additions.

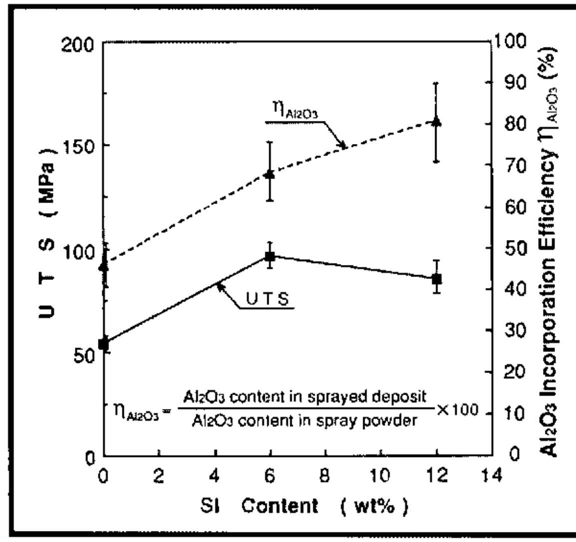

Fig. 18 — Increases in Si content improved the UTS and the Al_2O_3 incorporation efficiency.

Suggestion for Future Work

For comparison with some of the results in this report, several properties of the sprayed joints not containing SiC phase were investigated. Figure 27 shows the influence of Mg content in the spray deposit of ball-milled 2014 Al alloy on the joint strength. ß means the Mg/Si weight ratio calculated from the chemical analysis of each deposit. Precipitation of intermetallic compounds, such as CuA_{12} and Mg_2Si, by heat treatment provide significant improvement of the mechanical properties of 2014 Al alloy as values of ß approach 1.73. The joint with maximum strength in Fig. 27 was the strongest of the joints produced in this study — Fig. 28.

Kojima, *et al.* (Ref. 13), reported that in Al-Si-Cu-Mg alloys, the amount of Mg is reduced by 55% during plasma spraying. Therefore, though the standard Mg content in 2014 Al alloy is 0.8 wt-%, Mg contents adopted for the ball-milled powder of this experiment were 0.5, 1.5, 3.0, and 5.0 wt-%. Before spraying, unfortunately, the Mg content of the ball-milled powders was decreased about 56% because of adherence to the inside wall of the ball mill jar and the milling media due to use of fine Mg powder — Fig. 29. In addition, the Mg content decreased even further during plasma spraying as shown in Fig. 30. The resulting Mg contents are shown in Fig. 27.

As seen in Table 6, the higher the vapor pressure or lower the boiling point of the element, the larger the weight loss during plasma spraying. It was found that the sprayed Osprey deposit contained much soluble silicon (Table 6) and hence its value of ß was much less than the optimum of 1.73. Therefore, it is likely that a deposit with higher age-hardenability after plasma spraying can be produced. Hence, it is believed that an Osprey joint with excellent tensile properties might be obtained by better control of the amount of Mg in the deposit.

Ball-milled spray powders containing SiC particulates produced composite joints with lower strength and lower SiC phase content than those of the Osprey joints in this study. Thus it is preferable to make the composite powder by spray deposition rather than by ball milling. For production of composite spray powders by means of ball milling, it would be better to adopt longer periods of milling time to obtain a fully mechanically alloyed metal matrix and a highly homogeneous composite powder wherein the SiC phase is more uniformly dispersed in the soft alloy matrix.

In conclusion, future efforts should be directed towards the development of proper composite spray powder and the determination of optimum heat treatment conditions after spray joining.

Conclusions

General Conclusions

1) Plasma spray joining processes require preheating to obtain satisfactory results from joining. For Al deposits to 1100 Al substrates, 200°C was found to be an optimum preheating temperature.

2) The strength values of spray joints increased with increasing bevel angles.

3) Almost no Al_4C_3 phase was observed by XRD analysis in each sprayed deposit containing SiC phase, but the deposit contained much soluble silicon because of pyrolysis of some SiC particulates

4) Bonding between the reinforcement phase and the Al alloy matrix seemed to be very poor, especially for the larger volume fractions of SiC particulates.

Use of Al-Si-Ti Alloy Matrix Composite Powders

1) Although Ti additions had almost no effect on tensile strength of the joints,

Al-xSi-yTi-10vol%SiC(5μm)

y \ x	0	6	12	20
0.0	×	△	◎	○
0.5	△		○	
1.5	×	△	◎	○
3.0	△		◎	

Al-xSi-yTi-10vol%SiC(40μm)

y \ x	0	12	20
0.0	×	◎	◎
0.5	△	○	○
1.5	×	○	○
3.0	×	○	△

Al-xSi-yTi-10vol%Al2O3

y \ x	0	6	12
0.0	×	△	△
1.5	×	○	△
3.0	×	△	△

UTS (MPa)

◎ ········ 115 <
○ ········ 90-115
△ ········ 65-90
× ········ < 65

Fig. 19 Summary of the relationship between composition and UTS.

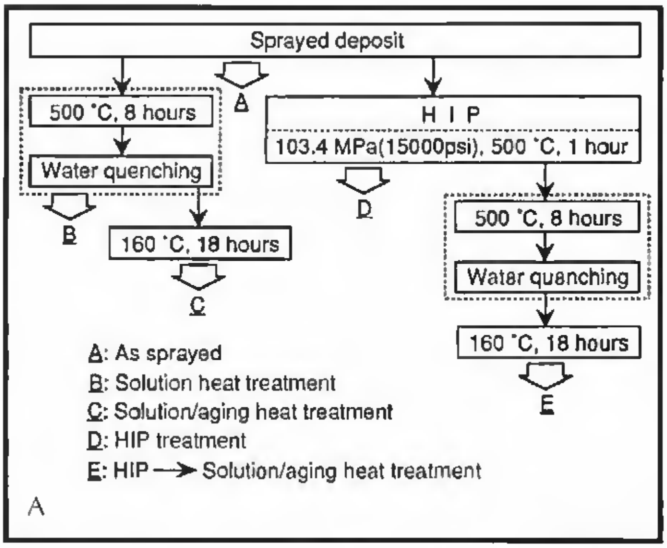

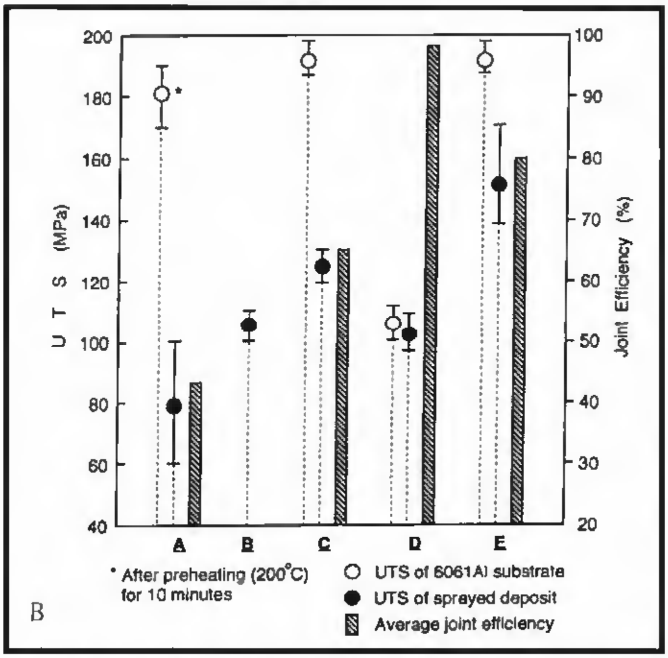

Fig. 20 — *Processing route describing the strengthening heat treatment of 2014 Al-15vol-%SiC for five different samples, A-E (Fig. 20A). Strength produced by various processing routes (Fig. 20B).*

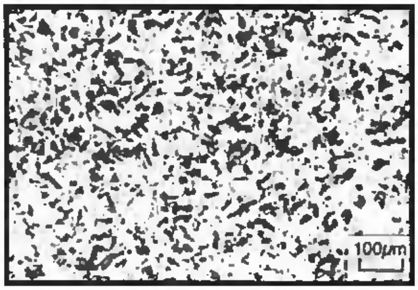

Fig. 21 — *Uniformity of dispersion and incorporation of Osprey deposit.*

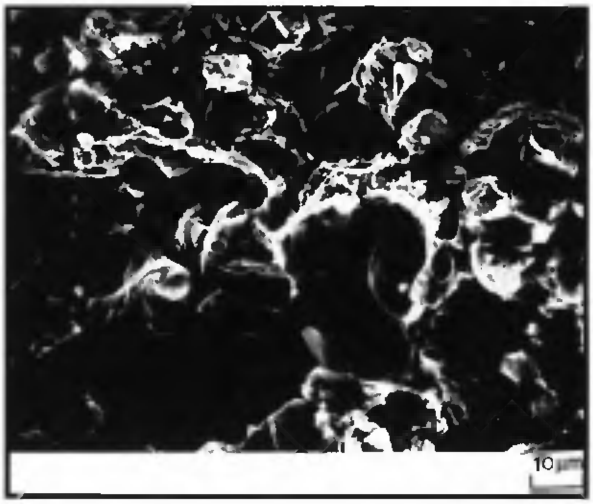

Fig. 22 — *Locally ductile, dimpled morphology was seen on the fracture surface of heat-treated Osprey powder deposits.*

Si was a very effective additive for all the composite powders. It was found that 12 wt-%Si for the composite powder with SiC particulates and 6 wt-%Si for composite powder with Al_2O_3 particulates were the best compositions to improve the joint strength.

2) Spray joints containing SiC were generally stronger than ones containing Al_2O_3 particulates.

3) The SiC content in the deposit was smaller than the Al_2O_3 content given an equal fraction of each in the starting powder. The Al_2O_3 content in sprayed deposits increased with the Si content.

4) Heat treatment seemed to improve the bonding at the interface of the substrate-deposit and/or the SiC phase-Al alloy matrix in the deposit. Since the deposit matrix did not contain alloys capable of providing precipitation hardening, the strength values of these deposits after heat treatment were not large

Use of 2014 A1 Alloy Matrix Composite Powders

1) All heat-treated joints were much stronger than as-sprayed joints. Most of them showed wholly cohesive failure mode, which means not only the deposit, but also the deposit-substrate interface were strengthened to a considerable extent by the heat treatment (T6).

2) The combination of HIP and T6 heat treatment caused the strength of the Osprey joints with unreinforced 6061 Al substrates to increase up to 95% compared with as-sprayed joints, but the results varied considerably from specimen to specimen.

3) The Osprey joints with SiC/6061Al and Al_2O_3/6061Al substrates were a little weaker than those with unreinforced 6061 Al substrates, and their strength values scattered widely. A HIP treatment prior to the T6 treatment of the joints with composite substrates was not so effective in improving the joint strength.

4) The strength of the joints made with ball-milled powders tended to decrease with increasing SiC content. Both the sprayed deposits with smaller SiC particulate (5 mm) and the Osprey deposits were stronger than those made with the ball-milled powders. The Osprey deposits showed a relatively high efficiency for incorporation of SiC (n = 70.3%).

5) Loss of Mg by vaporization during spraying upsets the ratio of alloy elements and produces joints which do not respond well to precipitation heat treatment. Special alloys which reduce such losses or tolerate them more readily should be developed to provide the

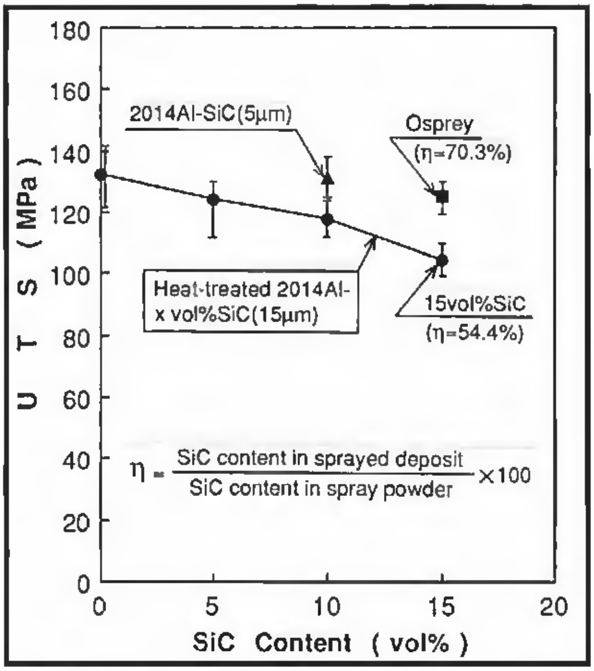

Fig. 23 — The strength of 2014 Al decreased with increasing SiC content for ball-milled powders.

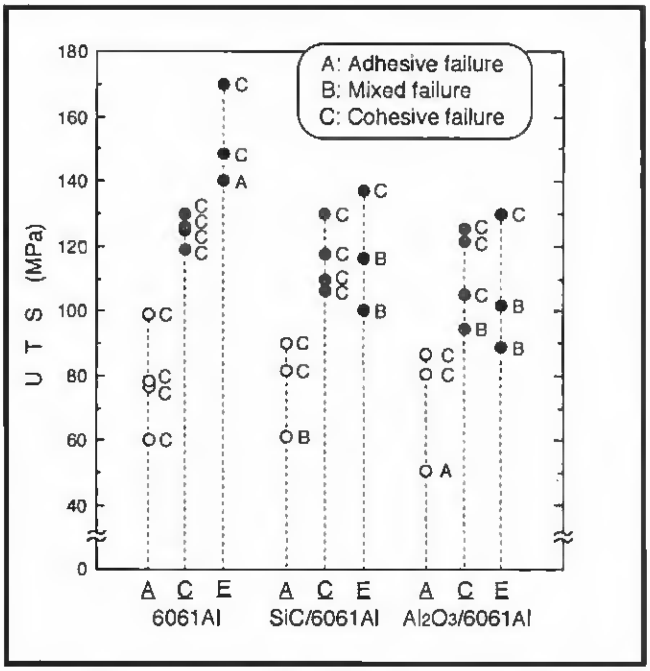

Fig. 24 — A comparison of results of strengthening treatments of the Osprey deposits on 6061 Al and 6061 Al matrix particulate reinforced substrates shows variations with heat treatment.

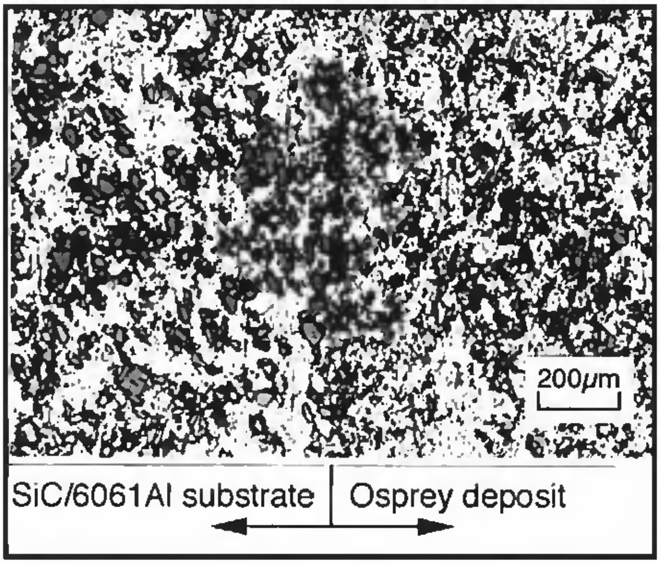

Fig. 25 — A change in particulate size can be seen across the deposit substrate interface for the SiC/6061 Al.

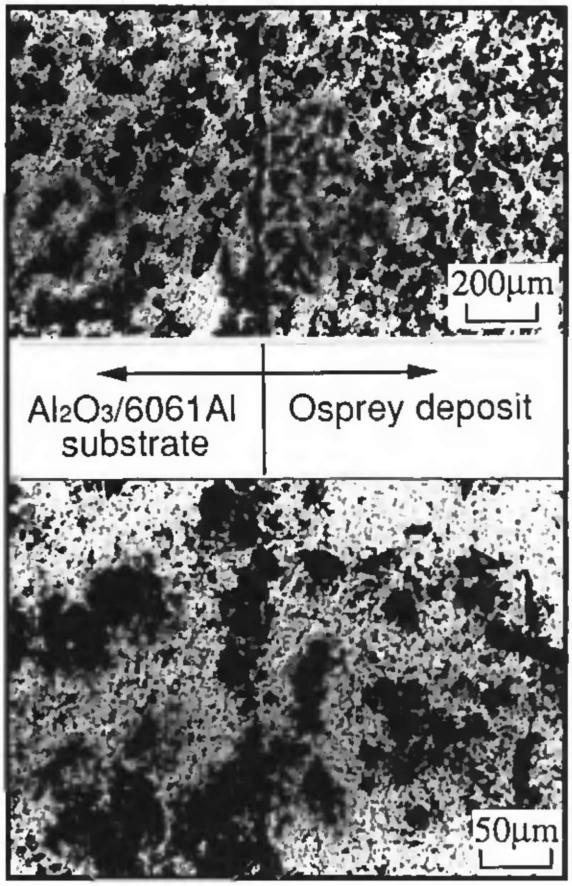

Fig. 26 — The deposit-substrate interface marks a change in particulate size and distribution for the Al_2O_3/6061 Al.

greatest joint strength in plasma sprayed and heat treated MMC.

Acknowledgments

The authors express their appreciation to Alcan Aluminum Co. for support of this work at MIT and to Rotary International, which supplied a fellowship for one of the participants (T. I.). Thanks are also due to Mr. Kiyoyuki Fukui, who provided some significant quantitative analysis data.

References

1. Ahearn, J. S., Cooke, C, and Fishman, S. G. 1982. Fusion welding SiC-reinforced Al composites. *Metal Construction* 14(4): 132-137.

2. Iseki, T., Kameda, T., and Maruyama, T. 1984. Interfacial

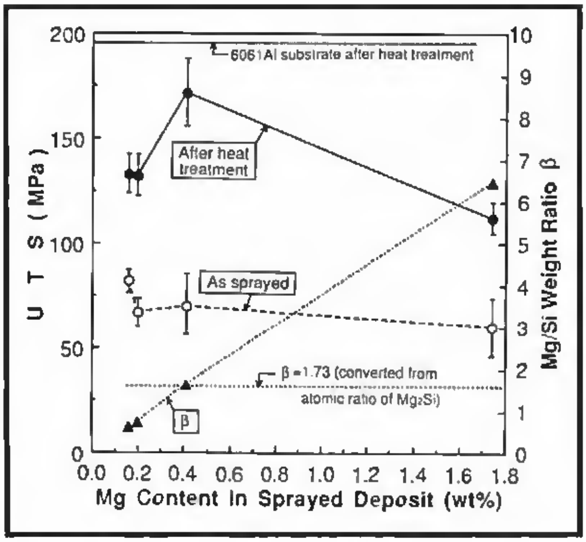

Fig. 27 — The highest joint strength was obtained at an optimum Mg/Si ratio.

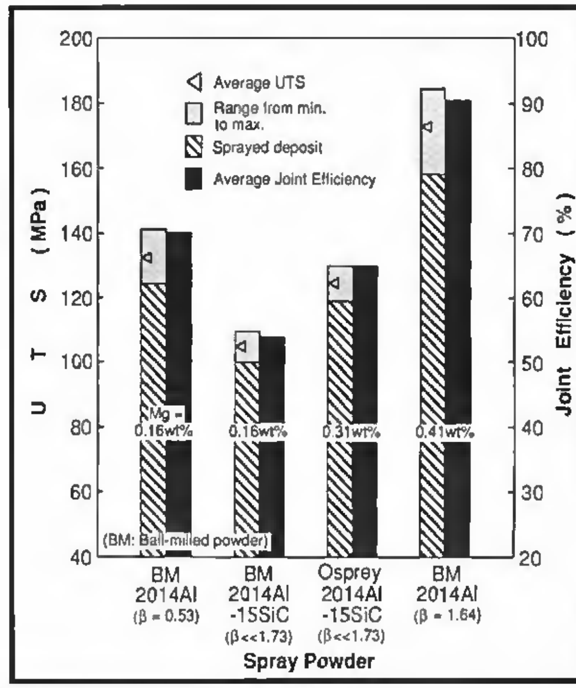

Fig. 28 — Comparison of ball-milled and Osprey powder joint strength.

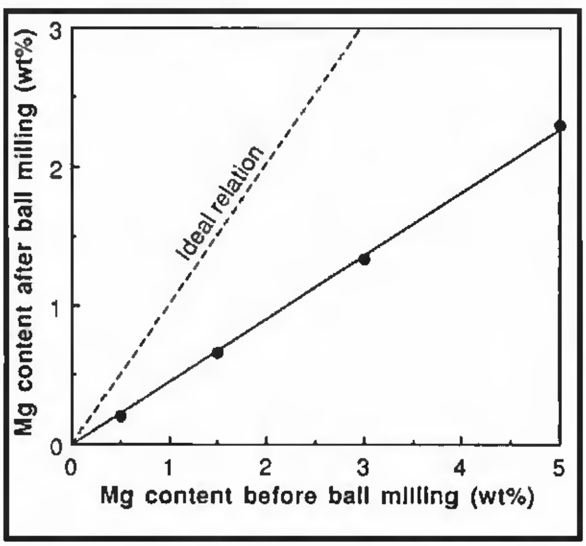

Fig. 29 — Magnesium content in composite powder was decreased about 56% during ball milling because of adherence of magnesium to the mill balls and walls.

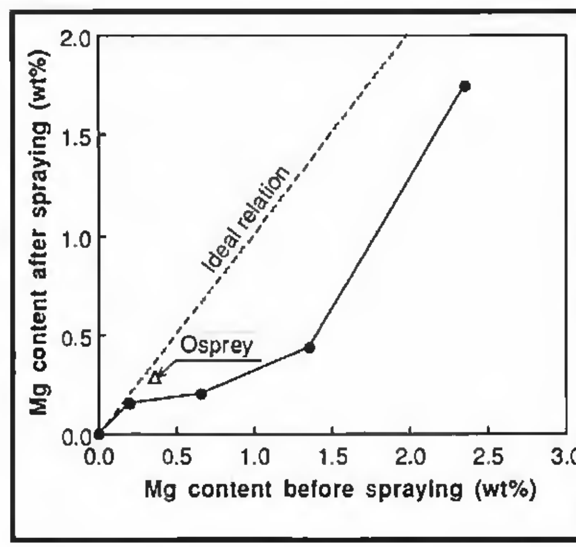

Fig. 30 — Magnesium was lost by vaporization during the spraying of the powder, resulting in reduced Mg contents.

reactions between SiC and aluminum during joining. *Journal of Materials Science* 13: 1632–1638.

3. Viala, J., Fortier, P., Bonnetot, B., and Bouix, J. 1986. High pressure interaction between solid Al and SiC. *Materials Research Bulletin* 21: 387–334.

4. Berndt, C. C., and Yi, J. H. 1987. Strength enhancement of plasma sprayed coatings. *Advances Coatings Technology*, pp. 237–308.

5. Laurent V., Chatain, D., and Eustathopoulos, N. 1987. Wettability of SiC by aluminum and Al-Si alloys. *Journal of Materials Science* 22: 244–250.

6. Yang, L. 1983. Thermodynamic analysis of factors controlling the microstructure of Al/SiC welds. Contract Number DAAG46-83-C-0023.

7. Courtesy of B. Altshuller, Kingston R&D Center, Alcan International Ltd.

8. *Plasma Spray Materials Handbook*, Bay State Abrasives.

9. *Metals Handbook*, 3rd Edition, 4, ASM Committee on Heat Treating of Aluminum Alloys, 673.

10. Fujiwara, C. 1986. Processing, microstructure and mechanical properties of silicon carbide particulate reinforced aluminum alloys. M.S. Thesis, Massachusetts Institute of Technology, Cambridge, Mass.

11. Suzuki, H., Kanno, M., and Shiraishi,Y. 1978. Effects of excess magnesium or silicon contents on the aging behavior of Al-1 .2%Mg2Si alloy. *Journal of Japan Institute of Light Metals* 28(5): 233.

12. Suzuki, H., Kanno, M., Shiraishi,Y. 1978. The age-hardenability of AlMg2Si alloys with excess silicon. *Journal of Japan Institute of Light Metals* 28(11): 553.

13. Kojima, Y. Mebata, A. , Sakamoto, M., and Onaka, N. 1988. Properties of low pressure plasma sprayed Al-Si, Al-Si-Cu-Mg alloy coatings. *Journal of Japan Thermal Spraying Society* 24(3): 1356.